ELSEVIER

Biochimica et Biophysica Acta 1368 (1998) 201–215

BIOCHIMICA ET BIOPHYSICA ACTA
BBA

Ultraflexible vesicles, Transfersomes, have an extremely low pore penetration resistance and transport therapeutic amounts of insulin across the intact mammalian skin

Gregor Cevc [a,*], Dieter Gebauer [a], Juliane Stieber [a], Andreas Schätzlein [b], Gabriele Blume [b]

[a] *Medical Biophysics, Clinics r.d.I., Ismaningerstr. 22, The Technical University of Munich, D-81675 Munich, Germany*
[b] *IDEA, Innovative dermal Applications GmbH, Frankfurter Ring 193a, D-80807 Munich, Germany*

Received 1 October 1996; revised 3 July 1997; accepted 14 July 1997

Abstract

New vehicles for the non-invasive delivery of agents are introduced. These carriers can transport pharmacological agents, including large polypeptides, through the permeability barriers, such as the intact skin. This capability depends on the self-regulating carrier deformability which exceeds that of the related but not optimized lipid aggregates by several orders of magnitude. Conventional lipid suspensions, such as standard liposomes or mixed lipid micelles, do not mediate a systemic biological effect upon epicutaneous applications. In contrast to this, the properly devised adaptable carriers, when administered on the intact skin, transport therapeutic amounts of biogenic molecules into the body. This process can be nearly as efficient as an injection needle, as seen from the results of experiments in mice and humans with the insulin-carrying vesicles. The carrier-mediated transcutaneous insulin delivery is unlikely to involve shunts, lesions or other types of skin damage. Rather than this, insulin is inferred to be transported into the body between the intact skin cells with a bio-efficiency of at least 50% of the s.c. dose action. © 1998 Elsevier Science B.V.

Keywords: Transfersome; Vesicle; Insulin

1. Introduction

Large biogenic or biotechnologic molecules are normally delivered into the body by means of an injection needle. However, numerous and ingenious attempts were made to improve on this [1,2]. They were based on inventive galenic formulations, including oral polymer [3], liposome [4] or microemulsion [5,6] suspensions, on the technical innovations, such as subcutaneous reservoirs [7] and pumps [8], or on the unusual, e.g. rectal [9], periocular [10], intranasal [11] or dermal [6] applications. None of these approaches to date gave completely satisfactory results.

The reasons for this are manifold. Orally applied polypeptidic or proteinaceous drugs are digested in the gastro-intestinal tract, by and large, and thus are therapeutically nearly inactive. Macromolecules placed in the nose or on the intact skin face the natural permeability barrier optimized by the evolution to keep the foreign substances out of the body; very few, if any, large entities therefore cross the intercellular passages in such barrier. What is the basic cause of this?

Pushing a large molecule or a particle through the

* Corresponding author. Fax: +49 89 4140 4980.

PII S0005-2736(97)00177-6

pore with diameter much smaller than the 'permeant' size is extremely energy-demanding, if not impossible; the molecular or particle segregation in the renal or sterile filtration, based on such size exclusion exemplifies this.

By using the concept of rational membrane design [12] we have recently devised special composite bodies, so-called Transfersomes [1] [13], which overcome the filtration problem: Transfersomes are sufficiently flexible to pass even through the pores appreciably smaller than their own size. By optimally matching the penetrant adaptability to the transport-induced stress the size-exclusion principle is evaded nearly completely. The resulting highly deformable vesicles then pass through the narrow, otherwise confining, pores with the efficacy of water, 1000 times smaller.

This article provides some evidence for this and also elucidates the mechanism of lipid aggregate penetration through various barriers in terms of vesicle local composition and shape adjustments. Our report, moreover, illustrates the use of highly deformable vesicles for the spontaneous transcutaneous delivery of drugs and discusses the practical value of such an approach.

2. Experimental

2.1. Permeation across an artificial barrier

Permeation across an artificial barrier was determined in a dedicated, home-built device. In short, the flux of vesicle suspension through a large number of pores of known size (e.g. through a sandwich of different micro-porous filters with the pore diameter between 50 and 400 nm, depending on the starting transfersome suspension) was driven by an external pressure (originally 3 MPa, later typically ≥ 0.5 MPa) and measured as a function of time. The relative permeation capability of the investigated suspension was then calculated by using standard hydrostatic-flow expression $\mathscr{P}_{\mathrm{Transf}} = j/\Delta p$, the result of calculation being calibrated relative to the corresponding value measured with the pure water (Permeation = $\mathscr{P}_{\mathrm{Transf}}/\mathscr{P}_{\mathrm{water}} \times 100\%$). The dynamic light scattering and HPLC were used before and after each experiment to control the degree of filtration and the changes in particle size.

2.2. Vesicle size determinations

The dynamic light scattering measurements were done in triplicate with a Zetasizer 2C instrument (Malvern Instruments, Malvern, UK). They were analyzed by the multi-tau procedure from an Autosizer software package.

2.3. Liposomes preparation

Liposomes consisting of soybean phosphatidylcholine (SPC) were prepared by the standard method. In brief, an organic solution of the required lipid mixture was first dried under vacuum (10 Pa) overnight. The resulting lipid film was then hydrated with triethanolamine–HCl buffer (pH = 6.5) to prepare a 10% lipid suspension. This suspension was sonicated for 60 min at 4°C until the desired vesicle radius was achieved. The latter was measured by the dynamic light scattering.

2.4. Transfersomes preparation

In short, transfersomes were prepared by mixing an ethanolic SPC solution with the appropriate amount of an edge-active molecule, such as sodium cholate. One kind of resulting charged suspension contained 8.7 wt% SPC and 1.3 wt% cholate as well as approx. 8.5 vol% ethanol, unless stated otherwise. Other biocompatible surfactants were used in different suspensions [38]. The suspension was subsequently mixed with triethanolamine–HCl buffer to yield total lipid concentration of 10 wt%. The resulting suspension was sonicated, frozen, and thawed (2–3 times) and brought to the desired size (as measured by means of photon correlation spectroscopy) by ultrasonication or intermediate-pressure homogenization. Vesicle suspension was ultimately sterilized by filtration through a 0.2 μm micro-porous filter (Poretics, CA, USA). The final vesicle size was confirmed by the dynamic light scattering.

[1] Transfersomes™: from the Latin 'transferre', to carry, and Greek 'soma', body.

2.5. Transfersulin preparation

Transfersulin preparation was based on a common pharmaceutical formulation of human recombinant insulin (HRI: Actrapid 100 or 45 HM; Boehringer-Novo, Mannheim, Germany). The starting insulin solution thus contained approximately 4 or 2 mg of polypeptide, and 3 mg (1.5 mg) *m*-cresol per ml. To prepare 1 ml of Transfersulin, 0.84 ml of the original solution was mixed, for example, with 88 mg of SPC and approx. 12 mg sodium cholate or an appropriate amount of other detergent (p.a.) in 0.1 ml ethanol. (In experiments with Actrapid 45 HM, the total lipid concentration was halved and the cholate concentration was increased by 10 mol%.) The resulting crude suspension was homogenized to yield a mixture of vesicles with a radius of approximately 90–110 nm. These transfersomes were then sterilized by filtration through a 0.22 μm pore filter (Sartorius, Göttingen, Germany) and used for experiments within the next 24 h. The final concentration of insulin in all transfersomal preparations was nominally 84 ± 2 U/ml or 40 U/ml. Other transfersome compositions are described in detail in Ref. [38].

2.6. Skin penetration and bio-efficacy tests in *vivo*

The total amount of the drug- or carrier-derived radioactivity in the body provided information on the skin penetration capability. For this purpose, phosphatidylcholine tritinurated in choline group and iodinated insulin were used. The former was incorporated quantitatively into lipid aggregates. The radioactive insulin was associated with carriers to ~90%. The concentration of these labels was measured in mice as described in our previous publications [37]. In brief, all blood and tissue samples were discolored with 0.4 ml H_2O_2 and 0.2 ml $HClO_4$ at 80°C overnight. Subsequently, the samples were neutralized with 0.2 ml CH_3COOH and 10 ml of Aquasol-2 (NEN-DuPont, Dreieich, FRG) was added. The total radioactivity was determined with a β-scintillation counter (Canberra-Packard, Dreieich, Germany) or with a γ-counter (Berthold, Wildbad, Germany).

The values assigned to the skin 'Surface' represent the sum of all counts from the stratum corneum strippings. Carcass means the residual body with the exception of the individually represented organs or tissues.

The whole body pictures were determined in the laboratories of Merck AG, by the courtesy of Dr. Steiner.

Transfersulin always contained the rapidly acting human recombinant insulin (Actrapid HM; Boehringer-Novo, Mannheim) at the given concentration. Blood glucose concentration was normally measured with a standard glucose-dehydrogenase blood glucose assay (Merck, Gluc-DH) in triplicate.

2.6.1. Murine experiments

Each experimental group consisted of 4–8 female NMRI mice (32 g, 8–12 weeks old) with manually trimmed hair. Mice were kept in individual cages and typically had the blood glucose concentration of 120 mg/dl after the fasting period of 6 h. This starting glucose level was determined by averaging the results of three separate values measured between $t = -2$ h and $t \leq 0$ h, but the day-to-day variability was up to 20%. At $t = 0$, Transfersulin (●), insulin associated with ethanolic (10%) phosphatidylcholine (PC) liposomes (○) or with phosphatidylcholine/bile salt (PC/BS, 65/35 rel. wt%, 7% ethanol) mixed micelles (◇) was applied on the test animals back (0.45 U/mouse) non-occlusively. 20 μl blood samples were collected from the tail end. The corresponding average (mean: y) blood glucose concentration always represents the net insulin-induced hypoglycemia. Its value was calculated as follows. First, the corresponding average result measured with the untreated or empty-transfersome treated animals, $\bar{y}_{\text{control}}$ (negative controls, ×), was subtracted from each individual glucose concentration value: $y(t) = y_{\text{uncor}}(t) - \bar{y}_{\text{control}}$. (The drift in the original data set for the latter two groups was essentially absent for $t \leq 4$ h but increased quasi-linearly to ≤20% during the following 12 h.) Second, the average value, $\bar{y}(0)$, of all data points measured at $t \leq 0$ was calculated (typically 3 per mouse, only 2 of which are shown in Fig. 4). Third, the relative concentration change was determined as: $(y(t)/\bar{y}(0) - 1) \times 100\%$.

Owing to the difficulty of hypoglycemia-experiments in mice the standard deviation of all experimental points was rather large; the extra uncertainty caused by the non-invasive use of Transfersulin only added the factor of 1.5 to this uncertainty.

2.6.2. Human experiments

After an initial test period (≥ 40 min), insulin preparations were uniformly smeared over the intact skin surface on the inner side of one forearm of healthy volunteers (60–80 kg, age 30–40, starting blood glucose levels between 73 and 85 mg/dl, fasting for 20 ± 2 h). 45 U of Transfersulin were typically used on an area 45–90 cm^2. In the early experiments, in which also the C-peptide was measured, blood samples (2–4 ml) were drawn every 10–30 min through a soft intravenous catheter placed in the other arm. In some experiments the catheter was flushed with 0.25 ml of heparin (2500 U) every 2–3 h without an observable effect on the experimental results. The first 0.25 ml of each sample (after heparin use 1 ml) were routinely discarded. Three independent samples were measured at least in triplicate, resulting in SD $\leq$ 3 mg/dl. In the latter experiments, which make out 20% of the represented data, the blood samples were drawn from a finger tip. They were processed by standard method mentioned above (in triplicate).

The epicutaneously used ethanol-containing liposomes (10%; PC/PG (9/1 M/M), 10% EtOH) or PC/BS mixed micelles (65/35 rel. wt%) with insulin and EtOH (7%) gave data represented by ○ and ◇ the corresponding 3-point average curves as – – and ———, respectively.

2.7. Insulin and C-peptide in the serum

The basal insulin level in normoglycemic humans is 2–20 U/ml; the basal level of C-peptide, a co-product of insulin secretion by the pancreas, is 0.2–2.5 ng/ml. This means that the serum C-peptide concentration normally exceeds that of insulin by the factor of 5, owing to different elimination times. Any significant deviation from the above mentioned value is indicative of the systemic delivery of exogenous insulin, for example, by means of Transfersomes. We therefore checked the change in the molar insulin/C-peptide ratio after epicutaneous Transfersulin administrations by radioimmunoassays. The used test kits were applicable in the range 1.5–500 μU/ml for insulin (Isotopen Diagnostics; CIS) and 0.1–20 ng/ml for C-peptide (Byk-Sangtic Diagnostics); all measurements were done in the endocrinological laboratory of the 3rd Medical Clinic, TU Munich, by courtesy of Prof. P. Botterman.

To facilitate the resulting data comparison, the average starting insulin concentrations for each individual experiment were normalized to the value of 6 μU/ml, that gives the average starting value of all experiments. Similarly, the starting C-peptide levels were normalized to 1 ng/ml. Insulin values $\geq$ 25 μU/ml (4% of the total data) were not considered, as it is believed that such high values (some in the range 100–500 μU/ml) were due to the sample contamination with the insulin from the skin.

2.8. The statistical significance

The statistical significance in the time-dependence curves of blood glucose was evaluated by assuming a Gaussian distribution for the blocks of data typically consisting of 20 individual values and then determining the 95% confidence limit.

To test the significance of the change in the serum insulin concentration the following procedure was used. Each insulin/C-peptide data-pair was first converted into the molar ratio. Subsequently, the change of the latter relative to the average starting value was individually calculated. This gave 230 data points which were combined and sorted according to time. 30 consecutive values were grouped and analysed assuming Gaussian distribution. This provided information on the variability of the average insulin/C-peptide ratio in the serum at each given time and the corresponding 90% confidence interval.

In other cases, Students *t*-test procedure from the graphical package ORIGIN (MicroCal, Amherst, MA) was used.

3. Results

In the following, our chief findings are presented in a logical sequence stressing the key issues.

Transepidermal water activity gradient can push the hydrophilic entities into and across the skin if their resistance to penetration is small enough. We have previously provided rather direct evidence for this claim, based on the results of animal studies [13]. More recently, computer simulations were done [15] and compared with the measured data (G. Cevc, G. Gompper, D. Kroll, D. Gebauer, to be

published), suggesting the following picture of spontaneous vesicle motion through a narrow pore.

A small driving pressure that acts on a soft vesicle (or, by inference, a much higher stress acting on a less flexible membrane) deforms the vesicle only little [15]. Vesicle consequently does not protrude deep into the pore and attains a locally stable conformation. Conversely, the vesicle that gets into a pore to a distance comparable to the pore radius profits appreciably from the lower potential energy (that is, from the higher water activity) inside the pore. Such vesicle then tends to be sucked into the pore spontaneously. When this happens, for example due to a spontaneous thermal fluctuation at the pore entrance, the permeability value becomes proportional to the driving force and permits relatively rapid vesicle motion across the pore [15].

Vesicle motion can be driven by an applied force but for the polar aggregates mainly the transdermal osmotic force, F_{trans}, is important when the suspension is administered non-occlusively. If so, the force magnitude is roughly proportional to the number of the osmotically sensitive molecules in each carrier: $F_{\mathrm{trans}} \propto n_{\mathrm{aggreg}}$. Small aggregates, such as mixed micelles, are thence less sensitive to the naturally occurring transepidermal hydration gradient than the larger bodies. The problem with the latter is, however, that they are normally excluded more efficiently from the pore.

Overcoming the size exclusion principle depends on the controlled lowering of the energetic cost for penetrant deformation. This can be realized by combining into a single entity two or more components with sufficiently different packing characteristics and 'spontaneous curvature'. This permits the resulting blend to change its composition transiently at the sites of large, and typically non-uniform, stress: the component which sustains the deformation better is accumulated while the less adaptable bilayer component is diluted at the maximally stressed site. Properly made and designed, composite ultradeformable bodies are therefore self-optimizing: their components flow between the sites of different deformation which ensures the high transfersome deformability. A direct consequence of this is the optimum pore-penetration capability of judiciously prepared mixed lipid vesicles.

To formalize this idea one can argue as follows. When the vesicle of radius r_{v} is pushed into a confining pore with the radius $r_{\mathrm{pore}} \leq r_{\mathrm{v}}$ work must be done to pay for the activation energy of the process, $G^{\#}$. This energy, in the simplest approximation, is proportional to the relative surface area of each vesicle, $(r_{\mathrm{pore}}/r_{\mathrm{v}})^2$ [13] and to the membrane elastic energy: $G^{\#}_{\mathrm{penetration}} \equiv \mathrm{G}^{\#} = \Delta G_{\mathrm{elast}}$. This elastic energy, in the simplest approximation, is given by the standard expression for the vesicle membrane deformability: $G_{\mathrm{elast}} = \kappa/2$ [16] and is roughly proportional to the square of (the relative) vesicle radius.

Anomalous membrane deformability can be modelled in terms of the stress-dependent rigidity factor, $\tilde{\delta}(c)$, which scales the elastic membrane energy, $G_{\mathrm{elast}} = \tilde{\delta}(c)\kappa/2$ [17], relative to the elastic energy of a standard membrane $G_{\mathrm{elast(standard)}} = \kappa/2$. When the value of $\tilde{\delta}(c)$ is low the energetic cost of elastic membrane deformation is also small. Membranes of low rigidity thus become extremely flexible under certain stress conditions. The resulting membrane-confined bodies, consequently, are strongly deformable in a stress-dependent manner.

To determine the relevance of aggregate adaptability in the process of the enforced permeation one can consider the logarithm of permeability value, which is inversely proportional to the corresponding activation energy:

$$\log \mathscr{P} \propto \exp\left(-G^{\#}/RT\right). \qquad (1)$$

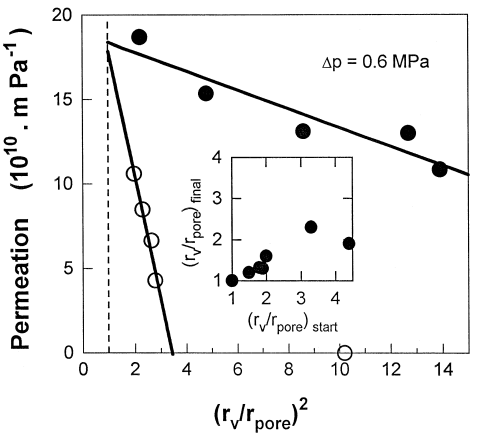

Fig. 1. The effect of relative particle size on the effective trans-barrier permeation of transfersome (2 wt% total lipid;) or liposome (2% PC;) suspensions driven by an external pressure, Δp. Inset: The average transfersome size after passage through the pores.

When this activation energy is sufficiently smaller than the thermal energy, $G^{\#}/RT \ll 1$, the above expression may be linearized

$$\mathscr{P} \propto \frac{1}{\tilde{\delta}\kappa}\left(\frac{r_{\mathrm{pore}}}{r_{\mathrm{v}}}\right)^2 \qquad (2)$$

to correlate the effective (dynamic) elasticity and deformability value, G_{elast} or $\tilde{\delta}(c)\kappa$ with the measured permeability in the systems with a known relative size ratio, $(r_{\mathrm{pore}}/r_{\mathrm{v}})^2$. Eqs. (1) and (2), moreover, permit the calculation of the average pore size from the $\mathscr{P}$-value if $\tilde{\delta}\kappa$ is known.

The elastic energy of liposomes is much higher than the thermal energy, $15RT \leq \kappa \sim 20RT$ [16,18]. Conventional vesicles are therefore too stiff to penetrate through the pores smaller than approximately 2 vesicle diameters (cf. Fig. 1, ○). Liposomes, consequently, do not cross the intact skin or get into the body (cf. Fig. 2, right). In contrast to this, Transfersomes, characterized by the high and nearly size-independent (cf. Fig. 1, ●) but stress-affected (cf. Fig. 2, ●) $\mathscr{P}$-value, can pass through the skin barrier nearly quantitatively (cf. Fig. 2, right panel).

By analyzing the data given in Fig. 1 by means of Eqs. (1) and (2) we infer that the observed transport capability difference is mainly due to the lower elasticity of liposomal in comparison with the transfersomal membranes. From the membrane surface fluctuations analysis (Gebauer and Cevc, to be published) we estimate that for transfersomes the average $\tilde{\delta}\kappa$ value is ≤ 1–$3RT$. The existence of the temperature induced, short-ranged surface fluctuations on the surface of typical Transfersomes, seen in the inset to Fig. 2, confirms the smallness of κ_{transf}.

The dynamic rigidity factor of transfersomes can be deduced from the stress-dependent permeability

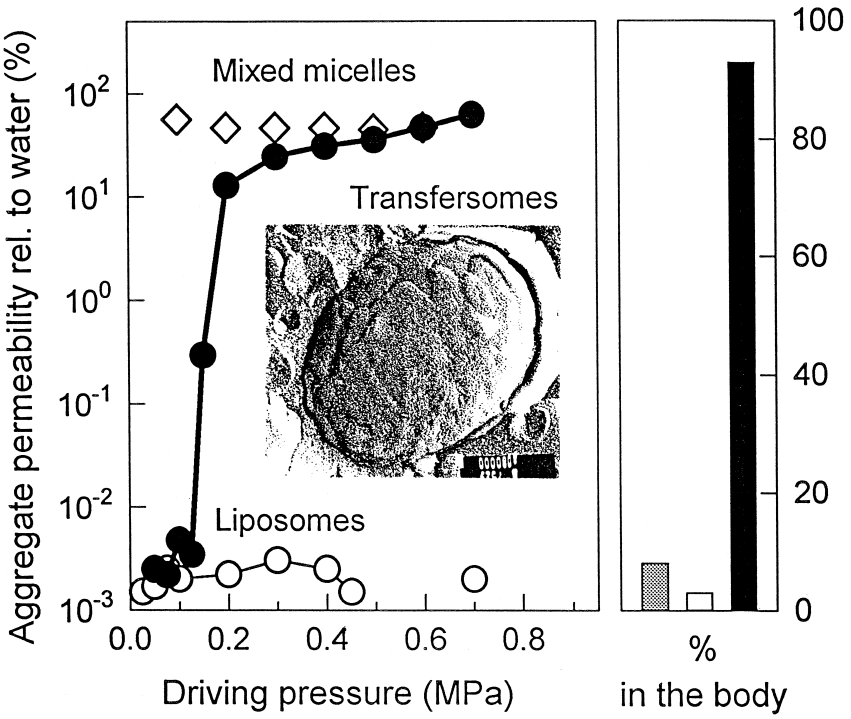

Fig. 2. Left: The relative permeability of the mixed lipid micelles (◇), transfersomes (●) or liposomes (○) as a function of the flow-driving pressure difference across the artificial barrier ($r_{\mathrm{pore}} = 200$ nm). All suspensions contained 2% total lipid and had compositions described in the text. The permeability values are given in % of the average value measured with water. Inset: A high magnification freeze-fracture electron micrograph of a large ($r_{\mathrm{v}} = 300$ nm), thermally undulated transfersome with $\kappa_{\mathrm{transf}} = \mathrm{RT}$. (Picture by courtesy of E. Sackmann and I. Sprenger, both TU Munich.) Right: the absolute efficacy of phospholipid transfer across the intact murine skin, as determined with the tritiurated dipalmitoylphosphatidylcholine, when this substance is incorporateed into mixed micelles (gray), liposomes (white) or transfersomes (black).

data as given in Fig. 2. To this end, the data measured with liposomes in the range of low permeation driving pressures are first used to fix $\tilde{\delta}^{\mathrm{def}} = 1$ for $\kappa_{\mathrm{lipos}} \simeq 20RT$ [18]. From the results obtained with transfersomes, for which one has $\kappa_{\mathrm{transf}} \rightarrow 1$, the rigidity factor for the optimized, composite vesicles is then estimated to be very small: $\tilde{\delta} \sim 0.07$. This value is sensitive to the penetration-driving pressure in the case of transfersomes, $\tilde{\delta}_{\mathrm{transf}} = \tilde{\delta}(\Delta p) \ll 1$, but not for liposomes.

Transition between the moderate and high permeation (or deformation) regimen occurs near $\delta p = 1.5 \times 10^5$ pa, when transfersomes (2% total weight) consist of phosphatidylcholine (PC, 1.695 wt%) and bile salt (BS, 0.305 wt%). In the low pressure region one gets for such typical suspension: $\kappa_{\mathrm{transf}} \simeq 2\text{–}5RT$

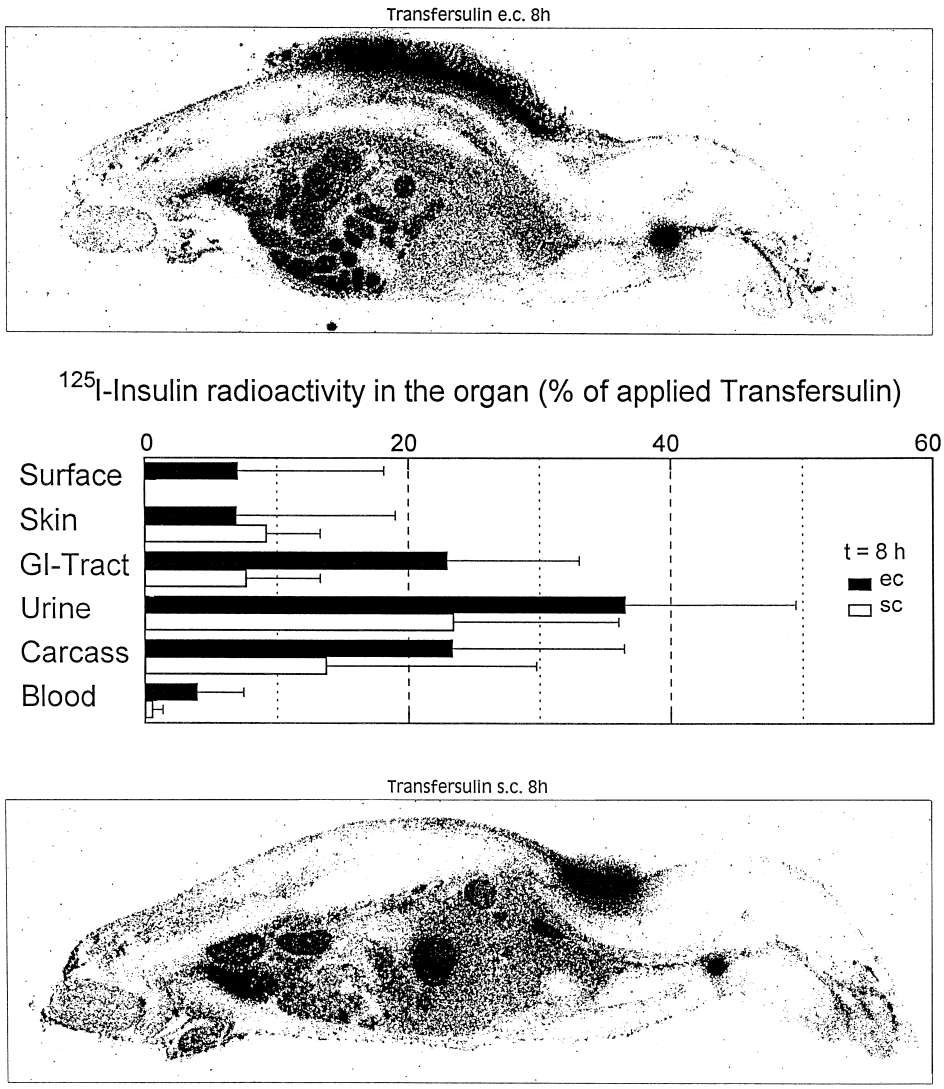

Fig. 3. Bio-distribution of the ^{125}I-insulin derived radioactivity in rats after an epicutaneous administration on dorsum (upper panel) or an injection under the dorsal skin (lowest panel). The middle panel gives the insulin-derived radioactivity distribution in mice ($n = 4$) 8 h after the epicutaneous administration of radio-labelled drug in Transfersomes. Owing to the lag-time of the transcutaneous insulin delivery the drug bio-distributions after e.c. and s.c. administration is not identical. Data likeness is sufficient, however, to prove that the ultradeformable carriers transport their associated drug into the body similar to the subcutaneous injection. Auto-radiographic pictures were done by the courtesy of Dr. Steiner from Merck AG; the upper one is blurred at the skin surface owing to the radio-label diffusion in the embedding matrix. For further details see the text.

and $\tilde{\delta} \sim 0.1$ whilst above $\delta p = 0.5$ mpa one has: $1 \sim \kappa_{transf} \leq 10^{-3} RT$ and $5 \times 10^{-3} \leq \tilde{\delta}(\Delta p) \leq 10^{-5}$. The upper limit estimate for $\tilde{\delta}$ stems from Fig. 1.

The high trans-barrier flow of transfersomes is due to the maximum stress-induced vesicle deformability rather than to the stress-induced vesicle fragmentation. This conclusion is directly supported by the fact that transfersome size is nearly the same before and after the pore passage (see the inset to Fig. 1) despite the shearing and transient bilayer ruptures during the crossing of pores. This is only strictly true for $r_v/r_{pore} \leq 3$–4, however, as larger transfersomes are too fragile to sustain strong shear-stress.

The same is true for the carrier-associated agents. Some 90% of the transfersome-associated insulin, for example, co-migrates with transfersomal carriers before and after the passage through a pore [19]. Simple lipid vesicles, liposomes, either break in the pore (cf. inset and Ref. [20]) or else are retained at the pore entrance (cf. Fig. 1).

Transfersomes are hence capable to transport agents across the biological barriers, such as skin. The match of the high membrane deformability and of the good carrier sensitivity to the transepidermal osmotic stress also maximizes the speed of carrier penetration through the skin [14]. Both permits the epicutaneously administered transfersomal drug formulations to induce a remarkable biological effect [21].

At first glance, this is surprising since the highly tortuous space between the horny-cells in the outer skin region is sealed nearly completely by the hydrophobic lipids [22]: the intercellular free-path width seldom amounts to more than a few tenths of a nanometer. Substances with a molecular weight higher than a few hundred Dalton, consequently, do not pass through the intact mammalian skin in significant quantity [23].

The skin permeability barrier is not uniform, however [24,25]. We have recently shown that it contains weak regions between the skin cells and, in particular, between the clusters of such cells. Through such 'virtual pores' the passage of the sufficiently potent penetrants can be enforced (A. Schätzlein and G. Cevc, paper in preparation and Ref. [26]). The effective diameter of an open virtual pore in the outer skin is around 30 nm. However, it must be kept in mind that normally only very few, if any, virtual pores in the skin are open. Similar conclusion was also drawn by others [27], who have suggested that the maximum pore size in the skin is around 20 nm, after the pores were opened during the enforced trans-epidermal material flow by means of iontophoresis.

Ultraflexible transfersomes described in this work are the first supramolecular agent carrier that can open and cross minute pores in the skin spontaneously [26]; the skin protruding pathogens are their natural, evolutionary optimized kin [28].

Transfersomes can transport their associated drugs, including the epicutaneously applied insulin, into the body spontaneously. This happens in spite of the fact that insulin is normally prevented from crossing the skin by its high molecular weight of 5808 Da.

We have proven this in animals as well as in humans. ^{125}I-insulin transfer across the intact skin and subsequent distribution of the insulin-derived radioactivity in the body, is demonstrated in Fig. 3. It is seen to closely resemble the result of an injection of the same amount, and kind, of formulation under the skin. While the middle panel gives the relative amounts of radioactivity in several relevant murine organs and in the residual body, the upper and lower panels illustrate the corresponding whole-body distribution patterns determined by means of auto-radiography in rats. Owing to the lag time of the transcutaneous drug delivery these patterns are not identical but sufficiently similar to support the above conclusion.

The representative results of the biological experiments with mice are illustrated in the top panels of Figs. 4 and 5. The epicutaneously administered, transfersome-associated insulin, Transfersulin (cf. Fig. 4, top: ●) from these data is seen to lower the blood glucose concentration by 20–30% within 2 to 4 h. In contrast to this, a mixture of insulin with the phospholipid/bile-salt micelles (◇) or a simple liposome/insulin blend (○) as well as empty transfersomes (not shown) do not change glucose concentration in the serum significantly over the investigated time period.

At $t \geq 4$ h the effects of animal fasting and manipulation in some experiments are manifest. The glucose concentration in the control mice now begins to vary (between $+10\%$ and -20% at $t = 8$ h). Glucose in the blood of all animals treated epicuta-

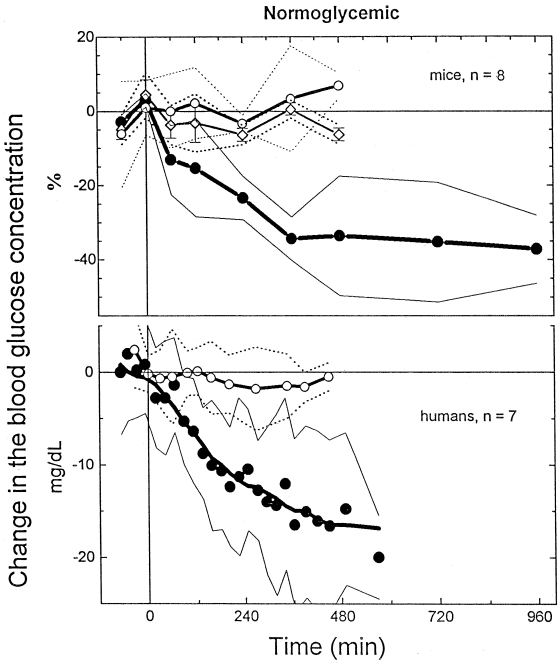

Fig. 4. The average glucose concentration change in the blood of mice (upper panel, in %) or humans (lower panel, in mg glucose per dl blood) as a function of time after the epicutaneous administration of Transfersulin (at $t = 0$). The thick curves run through the mean values and the thin, dashed or dotted lines define the corresponding 95% confidence limits for uncharged Transfersomes (●), charged liposomes (○) and mixed micelles (◇) as drug carriers, respectively. In mice, 0.45 U of insulin were used. The dose in humans was 0.6 U/kg in all cases. Experimental and formulation details are given in the text.

neously with the non-transfersomal insulin preparation shows the same trend and is essentially indistinguishable from the negative controls. For example, the liposomes-related data points given in Fig. 4 (top) do not differ from zero significantly at $t \leq 8$ h and the results obtained with mixed micelles deviate from zero only marginally (-3.8%, $P < 0.1$; not significant at $P < 0.05$) during a similar period of time.

This suggests that simple lipid suspensions or drug solutions do not deliver insulin across the skin. Of all the tested insulin formulations only the drug-laden transfersomes (Transfersulin) have this potential. Transfersomes deposited on the skin, moreover, act as an epicutaneous reservoir and prolong the hypoglycemic drug action. The surface density of the applied drug affects the pharmacodynamics of insulin action but does not abrogate the biological effect of Transfersulin in the dose range 0.5–2.5 mg/cm^2.

Transfersulin-induced decrease in the blood glucose concentration builds up with time. The net Transfersulin-induced hypoglycemia, defined as a difference between the treated group and the negative control, in mice typically exceeds 30% and sometimes approaches 50% of the initial blood glucose concentration at $t = 8$ h. This average concentration difference between the groups treated with Transfersulin and negative controls (zero by definition) is highly significant ($P > 0.001$) and amounts to approx. 30% of maximum hypoglycemic activity of the subcutaneously injected insulin at $t \simeq 1$ h (cf. Fig. 5, upper right).

Comparison of area under the curve is indicative of a high cumulative effect of the epicutaneously applied Transfersulin. In mice, this value reaches at least 50% of that resulting from an injection of Transfersulin (cf. Fig. 8, upper panel).

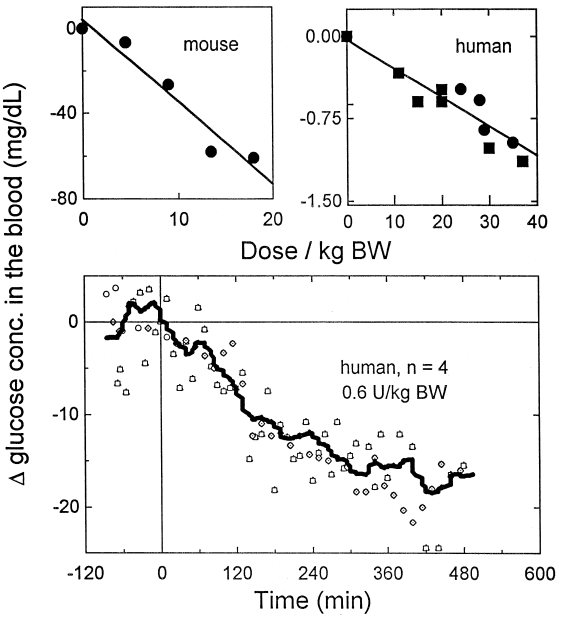

Fig. 5. Bottom: Characteristic suppression of blood glucose concentration in the normo-glycemic person after applications of insulin (0.6 U/kg body weight) in uncharged Transfersomes on the intact skin. The results from the individual experiments are shown as symbols and the corresponding mean value is given as a curve. Top: the dose vs. action curve determined in mice (left upper panel) or in a human (right upper panel). Lines in the upper two panels stem from a linear-regression analysis. In the human test person, Transfersomes of two different types were used. The murine data pertain to cardiac blood obtained after the killing of anesthetized mice at $t = 8$ h after the epicutaneous insulin administration.

Human data reveal a similar trend. Simple insulin-loaded liposomes (cf. Fig. 4, bottom: ○) or the corresponding mixed micelles (cf. Fig. 4, top: ◇) fail to induce significant hypoglycemia within the time period studied. Skin pre-treatment with a suspension of mixed micelles and the subsequent use of standard liposomes also is not efficient (data not shown). Only when insulin is applied in Transfersomes non-occlusively significant systemic hypoglycemia evolves. This happens at $t \geq 90-180$ min, depending on the detailed carrier composition. Such a delay of 45–145 min relative to the onset of the subcutaneous insulin action is at least partly due to the slower biological action of the carrier-associated drug [29].

The biological effect of insulin on the skin follows the same time-pattern and shows a similar delay in humans and in the hairy animals (cf. Fig. 4). This implies that pilosebaceous units do not act as an important transport shunt when the drug is delivered by means of Transfersomes.

During this study we found out that the transfersome-associated (bound) insulin is not readily detected by the standard immuno-assays done in a buffer (data not shown); insulin RIA will therefore have to be re-validated for Transfersulin in the future. The change in the serum insulin concentration after the administration of up to 0.6 U of the long acting drug per kg BW, moreover, only exceeds the detection limit by the factor of 4–5 [30]. This makes a reliable assessment of the systemic availability of insulin delivered by means of Transfersomes difficult. In order to get nevertheless some relevant information we used two procedures.

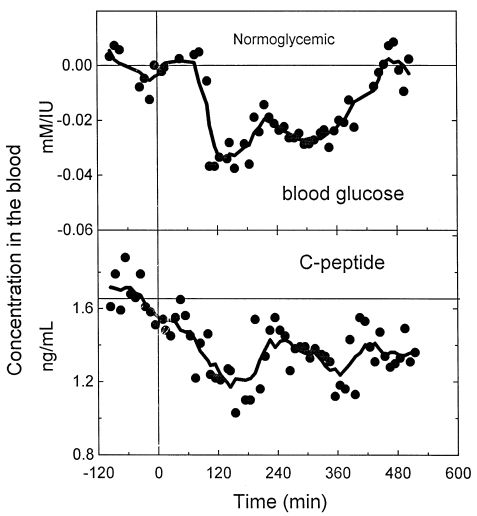

Fig. 6. Glucose (top) and C-peptide concentration (bottom) in the human blood as a function of the time after an epicutaneous administration of 0.5 U/kg of Transfersulin based on uncharged Transfersomes at $t = 0$. Curves were obtained by the nearest neighbor averaging.

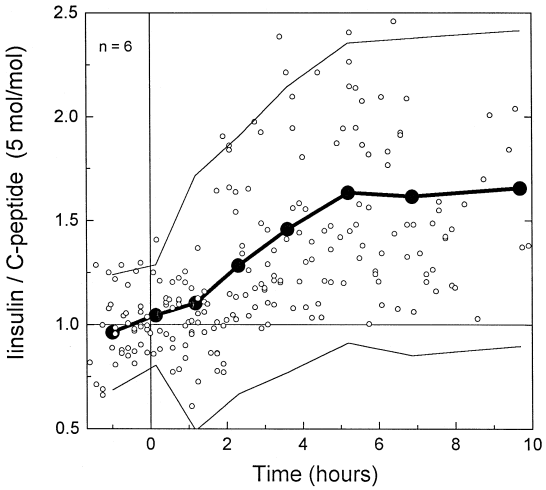

Fig. 7. The change in the systemic insulin/C-peptide molar ratio as a function of the time after epicutaneous Transfersulin administrations. Open symbols give the original data and bullets and thick curve the averaged results; thin lines define the 90% confidence interval. The large scattering in the original data set is either due to the physiological day-to-day variability or to the variations in the RIA-test performance, which could be caused partly by the interference from Transfersomes. On several occasions, the insulin level was also rather close to the detection limit and therefore not very reliable.

On the one hand, we tested the appearance of the epidermally administered insulin in the murine blood indirectly: we have used the ^{125}I-labelled drug (cf. Fig. 3) for this purpose. On the other hand, we also measured the insulin and C-peptide concentration in the blood as a function of time after the epicutaneous insulin application. Representative result of the former tests is given in Fig. 3. The outcome of the latter assay is illustrated in the bottom panel of Fig. 6 and in Fig. 7.

Data given in Fig. 6 were obtained with the formulation that combined intermediate and rapid drug action. They thus simultaneously illustrate the possibility to control the kinetics of Transfersulin action and document the interdependence of serum glucose and C-peptide, and thus insulin, concentration.

Data given in Fig. 7 represent the results of 6 experiments done on a non-diabetic test person with various amounts of different Transfersulin formulations. The individual data (not shown) indicate that the average insulin level remains fairly stable whereas the corresponding C-peptide level decreases markedly after the epicutaneous Transfersulin administration. Despite the large experimental scattering this confirms that Transfersomes deliver insulin through the intact skin. The most direct evidence for this is the 100% molar increase in the serum insulin concentration relative to the serum C-peptide level at later times. The simultaneous blood glucose depression also proves that the transcutaneously delivered insulin is biologically active (see Fig. 6 and compare Figs. 5 and 7).

4. Discussion

In brief, we report the following: the highly deformable agent carriers prepared from the self-optimizing mixtures of lipids may bring their associated agents through the biological permeation barriers, such as the intact skin. These novel drug carriers, so-called Transfersomes, provide means for the non-invasive transepidermal delivery of therapeutic agents. When loaded with insulin and applied in a reasonable quantity they induce therapeutically significant hypoglycemia in mice and in humans with a good efficacy and reproducibility. This offers new opportunities for the therapeutic use of large biogenic or biotechnological agents, such as peptides, on the intact mammalian skin.

To date, no unanimous answer has been found to the question of how and why could any entity as large as typical lipid vesicle ($MW \geq 10^6$ Da) cross the skin [31]. Many believe that this does not happen at all, owing to the high permeability barrier of the organ, which will only let molecules with a molecular weight lower than 500 Da, at the best, pass in significant quantity [23]. Other researchers would have us believe that the epicutaneously applied vesicles disintegrate in the skin and then bring their components with a poor efficacy into the body [31]. We have previously argued that large entities can trespass the skin if they are deformable enough to squeeze themselves between the skin cells through the otherwise confining pores [14].

Data given in Fig. 1 support our original assumption. They, moreover, confirm that the corresponding activation energy, in the first approximation, can be described within the framework of simple elasto-mechanics. This latter conclusion is directly corroborated by the linear relation between the permeability and the reciprocal (relative) vesicle area: ($\mathscr{P} \propto (1/r_v)^2$). The absence of appreciable vesicle fragmentation is supported by the constancy of the average vesicle size before and after the pore passage.

Permeability results measured with liposomes containing just one, relatively pure lipid (phosphatidylcholine) represent an upper-limit estimate for the value of $\mathscr{P}$(liposome). Two arguments speak for this. First, the observed liposome penetration through a pore with the diameter comparable to the vesicle size stems largely from the liposome size poly-dispersity (in our case: $\geq 25\%$); if a mono-disperse liposome suspension was used and there was no overlap between the vesicle- and pore-size distributions the actual $\mathscr{P}$-value probably would be much smaller. Second, the permeability of transfersomes with a relatively small r_v/r_{pore}-ratio is overestimated. Omitting the first measured data point from the linear regression analysis lowers the slope in the $\mathscr{P}$ vs. $(r_{pore}/r_v)^2$ line for the transfersomes by 40%. The bilayer rigidity factor, $\tilde{\delta}$, is proportional to this slope. For transfersomes, this factor thus is likely to be smaller than that given in the text: $\tilde{\delta} \leq 5 \times 10^{-3}$.

Permeation versus pressure curve pertaining to Transfersomes and illustrated in Fig. 2 is highly non-linear. We think that this is due to the rapid, stress-dependent increase in $\tilde{\delta}(\Delta p)$. This upholds our previous conjecture that the penetration of transfersomes through narrow pores is well regulated and self-optimizing: an excessive initial deformation-stress first decreases the value of $\tilde{\delta}_{transf}(\Delta p)$; this, in turn, reduces the deformation energy and minimizes the stress of penetration; $\tilde{\delta}_{transf}(\Delta p)$ then rises again, which increases the stress, etc. For a low driving pressure such changes are too short-lived to increase the vesicle penetration capability appreciably. In the range of high pressures, however, the resulting membrane deformability increase persists long enough to ensure transfersome flow through the 'confining pores' at maximum speed.

The self-regulating membrane deformability of transfersomes is closely related to the corresponding vesicles self-reparation capability, the latter being essential for the transfersome stability and practical usefulness.

To ensure the long-term colloidal stability of vesicular suspensions, the average elastic energy of each vesicle membrane must be higher than the thermal energy: $\overline{\kappa}_{\mathrm{transf}} \gg RT$. When this ceases to be true vesicles disintegrate spontaneously [32]. If membrane elastic energy is much higher, however, the resulting vesicles are too stiff to deform and sneak into a small pore. $\overline{\kappa}_{\mathrm{transf}} \sim RT$ compromises nicely between these two extremes: while it makes the membrane fluctuations probable (cf. inset to Fig. 2) it also maintains vesicle stability (cf. inset to Fig. 1).

In spite of this, the local elastic energy of a transfersome membrane may transiently get lower than RT. This happens, for example, when the vesicle rigidity factor is temporarily lowered at some strongly deformed site, $\kappa_{\mathrm{transf}}(\vec{r}) = \overline{\kappa}_{\mathrm{transf}}\tilde{\delta}(\vec{r}) \ll RT \leftrightarrow \tilde{\delta} \ll 1$, due to the stress-induced vesicle membrane adaptation. The non-linear pressure-dependence of transfersome passage through a micro-porous membrane (cf. Fig. 2) illustrates this functional dependence: for the low applied pressures the barrier permeability to the transfersome suspension is typically $> 10^4$ lower than for the pure water. At high pressures, the situation changes: the trans-pore flow of transfersomes now resembles that of water, 1000 times smaller.

High suspension-driving pressures nearly completely eliminate the effects of carrier- and pore-size mismatch. This is certainly true for the transfersomes with a diameter that does not exceed the pore size by more than the factor of 3.

Transcutaneous short-cuts, such as glands or hair-follicles, are known to play an important role in the process of molecular diffusion across the skin [23]. In spite of this, such shunts are either too sparse or too impermeable to let a large molecule, such as insulin, through the skin in appreciable quantity. This explains why an epicutaneous application of insulin in the mixed-lipid micelles or liposomes (cf. Fig. 4) has no significant hypoglycemic effect.

Shunts are also not crucial for the passage of transfersomes through the skin. If they were important, the biological action of the corresponding transepidermal drug administration on various animals or humans should differ considerably. This would manifest itself, in particular, in the variable onset of the insulin-dependent hypoglycemic action. Our experiments with mice (cf. Fig. 4), rats (cf. Fig. 3), pigs (not illustrated) and humans (cf. Figs. 4–6) exclude such a possibility. Indeed, to date, we were unable to detect any major pharmacodynamic difference between the various test species (mice, nude mice, rats, rat tails, pigs, humans) in spite of the fact that mice have at least 10-times higher hair-follicle density than pigs or humans.

Material transport into the skin could involve vesicle penetration through the cutaneous micro-lesions. This is unlikely to have played a role in our own experiments. If the skin was damaged and anomalously permeable to the insulin molecules, the corresponding transport increase should show-up in all tested formulations, but we only detected high transfer rates with transfersomes. The effects of skin lesions, if they did exist, moreover, should be mirrored in the increased inter-individual variability and the dependence of the experimental data-scattering on the mode of drug administration. In fact, the average standard deviations after subcutaneous injections and epicutaneous administrations are nearly the same, 18% and between 13% and 24%, respectively, for the single person data.

The last unpleasant possibility would be that our formulations were affecting the skin barrier directly. Bile salts, for example, are known to affect the permeability barrier of nasal mucosa [9,33]. Have such salts in our formulations also partly fluidized the skin and thus mediated a hypoglycemic insulin action?

If this were case, the measured decrease in the blood glucose concentration would have to increase, or at least remain constant, with increasing bile salt concentration. We observed just the opposite: the epicutaneously applied insulin/mixed micelles mixtures, which contain the highest bile salt concentration of all formulations studied, had no significant hypoglycemic effect (cf. Figs. 2 and 4).

We thus conclude that the reported hypoglycemic effect of Transfersulin is genuine. It is neither mediated by the skin-fluidization nor by the presence of skin lesions or merely the use of particulate carriers. Indeed, none of these factors seems to have played a

role in our experiments; the lack of hypoglycemic effect in mice treated with empty carriers, with an insulin solution or with the non-transfersomal insulin suspensions on the skin supports this conclusion. We infer that simple liposomes are insufficiently deformable to get across the skin and argue that micelles are too small to sense a strong enough transepidermal osmotic gradient to be driven across the skin.

The hypoglycemia measured after the non-invasive Transfersulin application, consequently, must be the result of transfersome-mediated drug transport across the skin. Our studies with the radioactive insulin support such conclusion ([19] and Fig. 3); so does the similar temporal dependence of C-peptide and glucose levels in the blood (cf. Fig. 6).

C-peptide is a side product of insulin bio-synthesis. If the measured hypoglycemia was not due to an epicutaneous Transfersulin action, but rather a response to the action of endogenic insulin, the serum C-peptide concentration in the blood should increase in parallel with decreasing blood glucose concentration. This should be true for the blood sugar concentrations higher than $\sim 60\,mg/dl$ at least. Our result show precisely the opposite trend, however. The similarity of time-profiles for the measured blood glucose (cf. Fig. 6, top) and C-peptide concentrations (cf. Fig. 6, bottom) thus provides a compelling evidence for the biological action of the exogenous, epicutaneously administered insulin in Transfersomes.

The lowest point in the systemic hypoglycemia measured after an epicutaneous Transfersulin application normally exceeds 25% and often reaches $45 \pm 10\%$ of the result generated by the corresponding subcutaneous Transfersulin injection (not shown). This only gives a lower-limit estimate for the total efficacy of the epidermally applied Transfersulin, however. Data shown in Fig. 8 reveal that the Transfersulin-mediated hypoglycemia actually persist much longer than that induced by a subcutaneous injection of Transfersulin [29]. Integration of individual hypoglycemia vs time curves suggests that the bio-availability of Transfersulin on the skin typically reaches 75% (cf. Fig. 8) and sometimes approaches 100% of the action of insulin under the skin [29].

Our results with Transfersulin thus supersede those of other previous non-invasive insulin applications. Even the best corresponding previous attempt, such as the use of iontophoresis [34] or trans-nasal spray [11,35], only brought less than 5% and less than 20% of insulin molecules, respectively, into the systemic blood circulation. The intra-pulmonal insulin administrations appears to be more efficient (up to 50%, [33,36] but is likely to be burdened by the poor administration reproducibility and also only gives rise to a short (2–4 h) hypoglycemia.

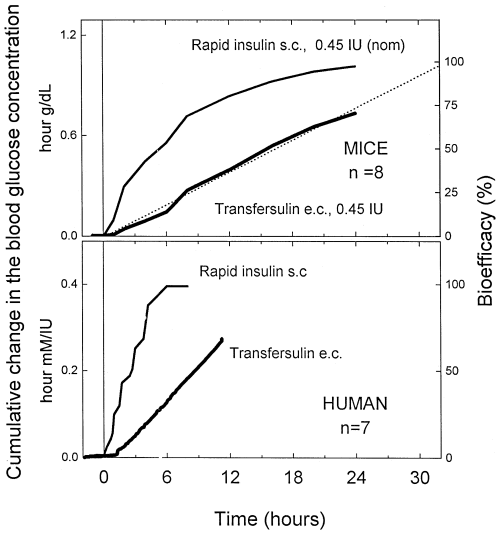

Fig. 8. Cumulative effect of the subcutaneously injected Actrapid ('Rapid insulin', thin curves) or of the corresponding amount of Transfersulin administered on the skin (thick curves) in mice (upper panel) or a human (lower panel). The results with human Transfersulin were obtained by calculating the area under the curve given in the bottom panel of Fig. 3 in Ref. [37]; curve labelled as 'Rapid insulin' in mice was obtained by the proper (3-fold) scaling of the data obtained after an injection of 0.15 U s.c., since the injection of 0.45 Actrapid in mice is lethal.)

The improvement over previous achievements calls for caution. Could it be that the blood glucose concentration in our experiments on human was changed by fasting? It stands to reason that this was not the case. If it was, the measured hypoglycemia should not be proportional to the drug amount used; the blood glucose level should never increase toward the end of experiments; the efficacy of each given preparation should be independent of carrier characteristics, etc. None of these implications is true, however (cf. Figs. 4–6).

Penetration of all properly made transfersomes is sufficiently controllable to ensure the insulin-induced hypoglycemia in mice and humans to be proportional

to the applied agent amount in the dose range below 0.2 U Transfersulin s.c./animal and below 0.6 U Transfersulin e.c./animal (cf. upper two panels in Fig. 5). In the normo-glycemic humans, dose linearity is observed below approx. 0.6 U Transfersulin e.c./kg (see the upper part of Fig. 5). The corresponding linear-regression analyses (straight lines) give correlation coefficients of $R = 0.96$ (■) and $R = 0.86$ (●) for mice and $R = 0.94$ for man and confirm that the observed effects are due to the non-invasively applied Transfersulin rather than to some other drug- or carrier-independent effect. The averaged results of measurements with humans before and after the onset of hypoglycemic area significant at the level of $P < 0.001$.

Transfersulin, in our experience, is reasonably efficient. In our experiments to date, the application area was varied between 20 and several hundred cm^2. It may be expected that, finally, Transfersulin will be administered over an area of merely 40 cm^2 or less to deliver the basal daily supply of insulin to a typical type I diabetes patient.

Hope is further nourished by the results of repeated experiments on one individual (cf. Fig. 5, bottom) with the optimized Transfersulin formulation which are clearly superior to our earlier data on a different test person [13]. The robustness of new results, together with the linearity of the dose vs. action curve, suggests that Transfersulin has, indeed, the potential to become a therapeutic formulation, provided that the batch to batch and the inter-patients variability can be made, or will turn out to be, small enough.

This demonstrates that it is possible to draw therapeutic benefits from the basic studies of elasto-mechanic properties of lipid vesicles and from the rational design of new quasi-biological materials.

Acknowledgements

This study was supported in part by the Deutsche Forschungsgemeinschaft (through the research grant Ce 9/1). We are thankful to the Central Animal Facilities of Gesellschaft für Strahlenforschung (Neu-Herberg b. M.), in particular to Dr. Griebel and Mrs. Möllenstädt for their generous hospitality. Technical assistance of Karin Putz in the experiments with mice is highly appreciated.

References

[1] M. Buysschaert, Optimized insulin delivery: achievements and limitations, Diabete Metabol. 15 (1989) 188–203.
[2] V. Lassmann-Vague, Unusual ways for administration of insulin, Diabete Metabol. 14 (1989) 728–731.
[3] M. Saffran, G.K. Sudesh, C. Savariar, J.C. Burnham, F. Williams, D.C. Neckers, Science 233 (1986) 1081–1084.
[4] N. Das, M.K. Basu, M.K. Das, Oral application of insulin encapsulated liposomes, Biochem. Int. 16 (1988) 983–989.
[5] Y.W. Cho, M. Flynn, Oral delivery of insulin [letter], Lancet 23-30 (1989) 1518–1519.
[6] R.K. Liedtke, K. Suwelack, K. Karzel, Wirkung peroraler und transdermaler Insulin-Praparationen auf die Blutglukose-Konzentration bei Mausen, Arzneim.-Forsch. Drug Res. 40 (1990) 880–883.
[7] P.Y. Wang, Implantable reservoir for supplemental insulin delivery on demand by external compression, Biomaterials 10 (1989) 197–201.
[8] H. Walter, A. Gunther, D. Kronski, I. Flaschentrager, H. Mehnert, Implantation of programmable infusion pumps for insulin delivery in type I diabetic patients, Klin. Wochenschr. 67 (1989) 583–587.
[9] B.J. Aungst, N.J. Rogers, E. Shefter, Comparison of nasal, rectal, buccal, sublingual and intramuscular insulin efficacy and the effects of a bile salt absorption promoter, J. Pharmacol. Exp. Ther. 244 (1988) 23–27.
[10] G.C.Y. Chiou, C.Y. Chuang, M.A. Chang, Systemic delivery of insulin through eyes to lower the glucose concentration, J. Ocul. Pharmacol. 5 (1989) 81–91.
[11] M. Mishima, S. Okada, Y. Wakita, M. Nakano, Promotion of nasal absorption of insulin by glycyrrhetinic acid derivatives, I. J. Pharmacobio.-Dynam. 12 (1989) 31–36.
[12] G. Cevc, Lipid properties as a basis for the modelling and design of liposome membranes, in: G. Gregoriadis (Ed.), Liposome Technology, 2nd ed., CRC-Press, Boca Raton, FL, 1992, pp. 1–36.
[13] G. Cevc, Material transport across permeability barriers by means of lipid vesicles, in: R. Lipowsky (Ed.), Handbook of Physics of Biological Systems, vol. I, Elsevier Science, Chap. 9, 1995, pp. 441–466.
[14] G. Cevc, G. Blume, Lipid vesicles penetrate into intact skin owing to the transdermal osmotic gradients and hydration force, Biochim. Biophys. Acta 1104 (1992) 226–232.
[15] G. Gompper, D.M. Kroll, Driven transport of fluid vesicles through narrow pores, Phys. Rev. E 52 (1995) 4198–4208.
[16] W. Helfrich, Elastic properties of lipid bilayers Theory and possible experiments, Z. Naturforsch 28 (1973) 693–703.
[17] S. Leibler, Curvature instability in membranes, J. Physique (France) 47 (1986) 507–516.
[18] D. Needham, E. Evans, Structure and mechanical properties of giant lipid (DMPC) vesicle bilayers from 20 Celsius

below to 10 Celsius above the liquid - crystaline phase transition at 24 degree Celsius, Biochemistry 27 (1988) 8261–8269.
[19] G. Cevc, G. Schätzlein, D. Gebauer, G. Blume, Ultra-high efficiency of drug and peptide transfer through the intact skin by means of novel drug carriers, transfersomes, in: K.R. Brain, V.J. James, K.A. Walters, (Eds.), Prediction of Percutaneous Penetration, 3rd International Conference, 14–16 April, 1993, Vol. 3b, STS Publishing, Cardiff, pp. 226–236.
[20] L.D. Mayer, M.J. Hope, P.R. Cullis, Vesicles of variable sizes produced by a rapid extrusion procedure, Biochim. Biophys. Acta 856 (1986) 161–168.
[21] P. Gonzalez, M.E. Planas, L. Rodriguez, S. Sanchez, G. Cevc, Noninvasive, percutaneous induction of topical analgesia by a new type of drug carriers and prolongation of the local pain-insensitivity by analgesic liposomes, Anesth. Analg. 75 (1992) 615–621.
[22] J. Hadgraft, R.H. Guy (Eds.), Transdermal Drug Delivery, Developmental Issues and Research Initiatives, Marcel Dekker, New York, 1989.
[23] R.O. Potts, R.H. Guy, Prediciting skin permeability, Pharm. Res. 9 (1992) 663–669.
[24] M. Fartasch, I.D. Bassukas, T.L. Diepgen, Structural relationship between epidermal lipid lamellae, lammelar bodies and desmosomes in human epidermis, an ultrastructural study, Br. J. Dermatol. 128 (1993) 1–9.
[25] E. Christophers, M. Schubert, C. Goos, The epidermis, in: M.W. Greaves, S. Shuster (Eds.), Pharmacology of the Skin, Vol. 1, Springer, Berlin, 1989, pp. 3–30.
[26] A. Schätzlein, G. Cevc, Skin penetration by phospholipid vesicles, transfersomes, as visualized by means of the confocal laser scanning microscopy, in: G. Cevc, F. Paltauf (Eds.), Phospholipids, Characterization, Metabolism and Novel Biological Applications, AOCS Press, 1995, pp. 191–209.
[27] V. Aguiella, K. Kontturi, L. Murtomäki, P. Ramírez, Estimation of the pore size and charge density in human cadaver skin, J. Control. Release 32 (1994) 249–257.
[28] A. Paul, G. Cevc, B.K. Bachhawat, Transdermal immunization with large proteins by means of ultradeformable drug carriers, Eur. J. Immunol. 25 (1995) 35221–35224.
[29] G. Cevc, Dermal insulin, in: M. Berger, F.A. Gries (Eds.), Frontiers in Insulin Pharmacology, Georg Thieme Verlag, Stuttgart, 1993, pp. 161–169.
[30] A.A. Starke, L. Heinemann, A. Hohmann, M. Berger, The action profiles of human NPH insulin preparations, Diabetic Med. 6 (1989) 239–244.
[31] H. Schreier, J. Bouwstra, Liposomes and niosomes as topical drug carriers, dermal and transdermal drug delivery, J. Control. Release 30 (1994) 1–15.
[32] R. Lipowsky, Vesicle thermodynamics, Nature 349 (1991) 475–481.
[33] D.T. O'Hagan, L. Illum, Absorption of peptides and proteins from the respiratory tract and the potential for development of locally administered vaccine, Crit. Rev. Ther. Drug Carrier Syst. 7 (1990) 35–97.
[34] B.R. Meyer, H.L. Katzeff, J. Eschbach, J. Trimmer, S.R. Zacharias, S. Rosen, D. Sibalis, Transdermal delivery of human insulin to albino rabbits using electrical current, Am. J. Med. Sci. 297 (1989) 321–325.
[35] R. Kimmerle, G. Friffing, A. McCall, N.B. Ruderman, E. Stoltz, J.C. Melby, Could intranasal insulin be useful in the treatment of non-insulin dependent diabetes mellitus?, Diabetes Res. Clin. Pract. 13 (1991) 69–76.
[36] L.L. Wearley, Recent progress in protein and peptide delivery by noninvasive routes, Crit. Rev. Ther. Drug Carrier Syst. 8 (1991) 331–394.
[37] G. Cevc, A. Schätzlein, G. Blume, Transdermal drug carriers, basic properties, optimization and transfer-efficiency in the case of epicutaneously applied peptides, J. Control. Release 36 (1995) 3–16.
[38] G. Cevc, 1991, Eur. pat. 91 114 163.8-2114.